NeuroImage **13,** 15–28 (2001)
doi:10.1006/nimg.2000.0680, available online at http://www.idealibrary.com on IDEAL®

Localization of Interictal Delta and Epileptiform EEG Activity Associated with Focal Epileptogenic Brain Lesions

Hans-Jürgen Huppertz,* Eberhard Hof,* Joachim Klisch,† Mirko Wagner,‡
Carl Hermann Lücking,* and Rumyana Kristeva-Feige*

**Department of Neurology and Clinical Neurophysiology and †Section of Neuroradiology, Department of Radiology, University of Freiburg, Breisacher Strasse 64, D-79106 Freiburg, Germany; and ‡Center for Data Analysis and Modeling, University of Freiburg, Eckerstrasse 1, D-79104 Freiburg, Germany*

Received February 10, 2000; published online November 3, 2000

The present study was aimed at investigating the accuracy of electric source reconstruction in the presurgical evaluation of epilepsy patients. Spontaneous EEG activity of 14 patients with focal intracerebral epileptogenic lesions was analyzed by source reconstruction based on high-resolution EEG (64-channel system) and a boundary element method head model accounting for the individual head anatomy. Equivalent dipole modeling was applied to focal delta and interictal epileptiform activity. The localization results were validated quantitatively by comparison with the sites of the structural lesions. In 6 of 9 patients with focal delta activity, the maximum of dipole concentration was closer than 10 mm to the nearest lesion margin and mostly at the border or within pathologically altered cortical tissue. In all 11 patients showing interictal epileptiform activity, the localization results were found in the same lobe as the lesion. In almost half of them, they were closer than 10 mm to the lesion margin. Patients with larger distances (22–36 mm) mostly had hippocampal atrophy or sclerosis. Their dipole locations did not appear in the affected hippocampus, but in the adjacent temporal neocortex. In conclusion, electric source reconstruction applied to both abnormal slow and interictal epileptiform EEG activity seems to be a valuable additional noninvasive component in the multimodal presurgical evaluation of epilepsy patients. © 2001 Academic Press

Key Words: **brain; brain mapping; electroencephalography; epilepsy; hippocampus; human; magnetic resonance imaging; methods; models; seizures.**

INTRODUCTION

In the presurgical evaluation of epilepsy patients, accurate localization of the epileptogenic focus is essential. Despite advances in structural imaging techniques, the functional localization by means of electrophysiological methods remains an indispensable part of the evaluation process. Seizure recordings using intracranial electrodes are regarded as "gold standard" for defining epileptogenic brain regions (Engel *et al.*, 1981; Spencer *et al.*, 1993). However, invasiveness, risk of morbidity, limited availability, and high costs of this technique limit its use in the clinical routine. The conventional interpretation of scalp-recorded electroencephalograms (EEGs), on the other hand, does not provide the localizing accuracy required for surgical planning. Only with the advance of more sophisticated analyzing methods, the information obtained from scalp-recorded EEG could be significantly increased. A growing emphasis has been on developing the method of electric source reconstruction based on equivalent dipole modeling (Henderson *et al.*, 1975; Cohen and Cuffin, 1983; Scherg, 1990). From the distribution of scalp-recorded EEG potentials and the shapes and conductivities of the different head compartments (e.g., brain, skull, skin), an inverse solution can be calculated for the location, orientation, and strength of possibly underlying sources. Recent advances include the coregistration of EEG data with anatomical information from magnetic resonance images (MRI) and the use of realistic head models (Gevins *et al.*, 1990; Roth *et al.*, 1993; Buchner *et al.*, 1995; Koles, 1998).

In the field of epilepsy, source reconstruction based on EEG and magnetoencephalography (MEG) has demonstrated its usefulness in localizing intracranial generators of interictal epileptiform activity (Ebersole, 1994; Baumgartner *et al.*, 1995; Diekmann *et al.*, 1998). The results were in agreement with those of other imaging modalities (MRI, positron emission tomography, or intracranial EEG recordings (Nakasato *et al.*, 1994; Stefan *et al.*, 1994; Roth *et al.*, 1997; Merlet *et al.*, 1998)). In addition, the propagation of interictal spikes has been studied (Wong, 1993; Ebersole, 1994; Baumgartner *et al.*, 1995). Other investigators have focused on locating abnormal low-frequency neuromagnetic activity as a marker of regional cortical dysfunction associated with epileptogenic lesions (Vieth *et al.*, 1996; Gallen *et al.*, 1997).

1053-8119/01 $35.00

The accuracy of localizing electric sources noninvasively has been assessed previously (Cohen *et al.*, 1990; Cuffin *et al.*, 1991): Artificial dipoles generated in human brains with implanted depth electrodes could be located with an average error of 10 to 11 mm. Using a human skull phantom the average localization error was even smaller (7–8 mm for EEG and 3 mm for MEG (Leahy *et al.*, 1998)). The reproducibility of source reconstruction based on high-resolution EEG of the N20 SEP component was found to be in the range of 2.6 to 4 mm (Kristeva-Feige *et al.*, 1997). However, there have been only a few studies quantifying the accuracy of source reconstruction in the presurgical evaluation of epilepsy patients. Using MEG source analysis, Stefan *et al.* (1994) could locate focal epileptiform activity to within 10 mm of the border of seizure-related tumors. With a combined EEG/MEG approach, Diekmann *et al.* (1998) found the calculated locations of interictal spikes in an average distance of 18 mm to epileptogenic lesions. Krings *et al.* (1998) located interictal spike activity or rhythmic EEG activity at seizure onset to within 8 mm of the border of epileptogenic lesions.

The present study was aimed at investigating the accuracy of electroencephalographic dipole localization in a series of 14 epilepsy patients with focal epileptogenic lesions. Two approaches were used: electric source reconstruction applied to (1) focal delta EEG activity, suggested to be a marker of regional cortical dysfunction associated with epileptogenic lesions (Gambardella *et al.*, 1995; Vieth *et al.*, 1996; Gallen *et al.*, 1997), and to (2) interictal epileptiform activity, generated in the irritative zone according to Lüders *et al.* (1993).

The results of electric source reconstruction were validated by comparison with the sites of the structural lesions. Consequently, the study also addressed the relationship between epileptogenic lesion and irritative zone in symptomatic focal epilepsy. In contrast to the above-mentioned studies (Stefan *et al.*, 1994; Diekmann *et al.*, 1998; Krings *et al.*, 1998), the electric source reconstruction was based on a high-resolution EEG (64-channel system) and a realistically shaped boundary element head model which is expected to be more accurate than the usual three- or four-shell sphere models (Yvert *et al.*, 1997). The results of the present study have implications on assessing the value of electric source reconstruction in the presurgical evaluation of epilepsy patients.

MATERIALS AND METHODS

Patients

Fourteen epilepsy patients (10 males, 4 females, 25–74 years) were selected from the routine clinical EEG laboratory according to the following criteria: (1) EEGs with focal delta activity and/or interictal epileptiform activity (spikes, sharp waves) and (2) one focal lesion on MRI which was regarded as epileptogenic according to clinical reasoning considering the semiology of seizures and the localization of interictal epileptiform activity in the EEG. Patients with multiple lesions or diffuse pathology on MRI or multiple focal slowing in the EEG were excluded. Informed consent was obtained from each patient.

High-Resolution EEG

Using a 64-channel EEG system (Neuroscan), the EEG was recorded from 61 scalp electrodes equally distributed over both hemispheres, including two subequatorial electrodes to improve localizations in the temporal lobe (Cz electrode as reference; ground electrode on the forehead; electrode resistances below 5 kΩ). Eye movements and blinks were monitored to exclude artifacts. The measurement protocol consisted of 15-min recording of spontaneous EEG activity (i.e., without hyperventilation, photostimulation, withdrawal of antiepileptic drugs, or drug-induced activation) in a HF-shielded room (bandpass filter 0.1–100 Hz, sampling rate 500 Hz).

For subsequent EEG/MRI coregistration, the electrode positions were digitized using an ultrasound localizing device (Zebris) and the head contour was obtained by collecting approximately 1600–2000 points while moving the digitizer across the head surface.

Analysis of Delta EEG Activity

The EEG data processing was done offline (Neuroscan software Scan 3.0). If focal delta EEG activity was established by visual inspection, the EEG was digitally filtered in the delta range (bandpass filter 1–3.5 Hz, 24 dB/Oct, zero phase shift).

A principal component analysis (PCA) based on a singular value decomposition algorithm (1992) was used to select periods of time showing one predominant component in the filtered EEG. This was done because the single equivalent dipole model used in the subsequent source reconstruction is only adequate for describing EEG data with one predominant underlying source (Kober *et al.*, 1992; Vieth *et al.*, 1996). The PCA analyzed the filtered EEG in time epochs of 480 ms with an overlap of 160 ms. The EEG data were decomposed into multiple linearly independent, i.e., temporally and spatially noncorrelated "principal components" (Soong and Koles, 1995; Friston *et al.*, 1996; Lagerlund *et al.*, 1997). An EEG epoch was accepted if the first component was at least 10 times higher than the "noise floor" of the four components following in strength. As an example, the PCA results of two EEG epochs are plotted in Fig. 1, one containing no predominant principal component and the other showing a high component followed by a noise floor consisting of

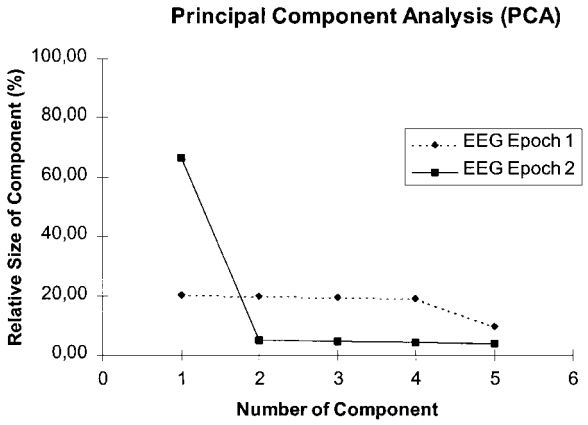

FIG. 1. Example of PCA results of two EEG epochs. The principal components are ordered by their strength. The first EEG epoch contains no predominant principal component (dotted line), while the second one shows a high component followed by a kind of "noise floor" consisting of components 2–5 (solid line).

component 2–5. Apparently, one component is dominating in the second epoch. Although there is no one-to-one correspondence between principal components and individual sources, an EEG epoch with one predominant underlying source can be expected to go along with one predominant principal component (Vieth *et al.,* 1996; Lagerlund *et al.,* 1997). Typically, about 30 s were selected out of the original 15 min of EEG, imported into the source reconstruction software (CURRY, Neuroscan) and rereferentiated to a common average reference.

Analysis of Interictal Epileptiform Activity

Spikes and sharp waves were identified visually according to IFSECN criteria (Chatrian *et al.,* 1974) and marked on the highest negative peak in the EEG (Neuroscan software Scan 3.0). If there were different types of spikes/sharp waves separable by their waveform or scalp distribution, they were collected in different groups. Only groups containing three or more epileptiform events were admitted for further analysis.

MRI and Surface Segmentation

A 3D anatomical data set was acquired using a MPRage sequence (TR/TE/alpha = 9.7 ms, 4 ms, 12°) on a 1.5-T Magnetom Vision (Siemens). With 256^2 pixel per matrix, 170 slices, a field of view of 256 mm, and a 3D slab thickness of 170 mm, the resulting voxel size was 1 mm^3.

Based on the MRI data, four different surfaces were segmented (CURRY software, Neuroscan): (1) *Cortex:* A semiautomatic 3D region growing algorithm started from inside the brain and stopped at the border between the white and gray matter (gray scale threshold criterion) (Wagner *et al.,* 1995). In critical regions (e.g., orbita, temporal pole) "boundary markers" were inserted. The finally segmented cortex surface consisted of about 20,000 triangles. (2) *Inner skull:* The segmentation was achieved by smoothing and expanding the segmented cortex surface. (3) *Outer skull:* The segmentation was performed by expanding the inner side of the skull. (4) *Skin:* After setting all gray values inside the outer skull to white, the skin surface was segmented by a region growing algorithm searching from inside for the border between skin and surrounding space. To the lower end of the head the surface was limited by an artificial border.

Coregistration of EEG and MRI Data

The coregistration of EEG and MRI data, i.e., the transformation of electrode positions and MRI data into the same coordinate system, was based on matching the digitized head surface as obtained by 3D ultrasound scanning after each EEG recording and the head surface as segmented from the MRI data (Huppertz *et al.,* 1998).

Electric Source Reconstruction

An inverse solution algorithm based on a single equivalent current dipole (ECD) model (Henderson *et al.,* 1975; Cuffin, 1985; Scherg, 1990) was applied for electric source reconstruction (CURRY software, Neuroscan). For a given time point, this algorithm iteratively minimized the difference between the measured EEG scalp potentials and the theoretical potential distribution which a single dipolar electric source in the brain, i.e., the ECD, would generate. The goodness of fit (GoF) was determined as the percentage of EEG data explained by the solution of the ECD location.

The source reconstruction was calculated in individual head models using the boundary element method (BEM) (Gevins *et al.,* 1990; Roth *et al.,* 1993; Buchner *et al.,* 1995; Koles, 1998) and accounting for the realistic shape of the three compartments, skin, skull, and brain (including the surrounding cerebrospinal fluid). The surfaces of these compartments were segmented as described above. The conductivities of the different tissues were defined as 0.33 S/m for the skin, 0.0042 S/m for the skull, and 0.33 S/m for the brain (Geddes and Baker, 1967). A separate compartment representing the cerebrospinal fluid was not defined because of potential mathematical errors arising from closely spaced boundary surfaces in a BEM model, in this case the surfaces of brain and cerebrospinal fluid (Fuchs *et al.,* 1998). Due to the same reason, the source space defined as the brain (+ cerebrospinal fluid) compartment was reduced by 3 mm in a closing operation.

EEG epochs with delta activity as selected by PCA were subjected to an automatic electric source reconstruction which analyzed the data in steps of 4 ms and collected location results with a GoF $\geq$ 85% (Boon and D'Have, 1995). To summarize the results of all EEG

epochs, a spatial dipole density distribution was calculated (Vieth *et al.*, 1993; Diekmann *et al.*, 1998). The 3D MRI data set was divided in voxels of 3-mm edge length. For each voxel, the number of ECD locations within this voxel was counted and a dipole density was calculated which was standardized in relation to the volume of the source space and the sum of all localized ECDs. For example, a dipole density of 100 meant that 100 times more dipoles were located in the analyzed voxel than in case of an equal distribution of localization results within the source space of the respective patient. The dipole density distribution was encoded in squares of different sizes which were projected onto the 3D representation of the segmented cortex at the site of the corresponding voxels.

Epileptiform discharges were analyzed in two steps. First, electric source reconstruction was applied to each *single* epileptiform discharge. Only epileptiform events with a GoF $\geq$ 85% were considered and averaged. If there were events belonging to different groups of similar spikes or sharp waves, they were averaged separately. Then, electric source reconstruction was applied to the peak of the *averaged* epileptiform discharges. The resulting ECD location was projected onto the 3D representation of the segmented cortex and depicted in the appropriate MRI slices.

Evaluation of Localization Results

The results of source reconstruction were validated by comparison with the site of the MRI-verified structural lesion in each patient. As a measure of the goodness of localization, the distance between the lesion and (1) the maximum of the dipole density distribution (resulting from the analysis of the delta EEG activity) and/or (2) the ECD location of the averaged interictal epileptiform activity was calculated. The distances were determined by two independent investigators (J.K. and E.H.) using the CURRY software.

RESULTS

Source Reconstruction of Delta EEG Activity

Nine of 14 patients showed intermittent or continuous focal delta EEG activity. In all but 1 patient, the maximum of dipole density was located in the same hemisphere as the MRI-verified lesion. In 6 patients (67%), the maximum was closer than 10 mm to the nearest lesion margin. Four of these patients (44%) had the maximum at the immediate lesion border or within pathologically altered cortical tissue (Table 1).

In four patients, more than one maximum of dipole density was observed: One patient with hippocampal sclerosis (patient 5) showed three equal maxima close together in the posterior part of the middle orbital gyrus and adjacent to the parahippocampal gyrus. The center of gravity of these maxima was located 17 mm from the affected hippocampus. Another patient with an infarction of the right middle cerebral artery (patient 11) had two equal maxima, one in the precentral gyrus (within 3 mm of the infarct margin) and the other in the postcentral gyrus (at the infarct margin). In the third patient who also had an infarction of the right middle cerebral artery (patient 10), three equal maxima were found close together in the right angular gyrus along the infarct margin. The fourth patient (patient 2) showed four equal maxima lying in the gray and white matter along the interhemispheric fissure. The minimum distance to the lesion was 46 mm and thereby far beyond the results of the other patients. It is noticeable that his high-resolution EEG displayed only rare and flat delta waves.

In a patient with right hippocampal atrophy (patient 9), the maximum of dipole density was found in the contralateral uncus hippocampi, while the averaged interictal epileptiform activity was located in the ipsilateral inferior temporal gyrus.

Source Reconstruction of Interictal Epileptiform Activity

In all 11 patients with sufficient interictal epileptiform activity (number of averaged spikes or sharp waves varying between 3 and 8, average 5), the ECD location of the averaged interictal epileptiform activity was located in the same lobe as the MRI-verified lesion. The corresponding GoF values varied between 93.1 and 98.7%. In 5 patients (45%), the ECD locations were closer than 10 mm to the nearest lesion margin (Table 1).

Four patients showed a relatively large distance (22—36 mm) between source reconstruction results and nearest lesion margin. Three of them (patients 3, 4, and 9) had a hippocampal atrophy or sclerosis. Their location results did not appear in the affected hippocampus, but in the adjacent temporal neocortex, i.e., the inferior temporal gyrus, or middle occipitotemporal gyrus. The fourth patient had a venous malformation with gliosis of adjacent white matter in the right parietal lobe (patient 13). The ECD location was deep in the white matter and near the trigonum of the lateral ventricle.

Results of Selected Patients

Patient 1. This 29-year-old man had simple-partial seizures with Jacksonian march of convulsion in the right arm and secondarily generalized tonic–clonic seizures. In the past, he underwent several embolizations and a partial operative removal of an arteriovenous malformation in the left temporoparietal and insular

TABLE 1

Principal Diagnoses, Lesion Sites, and Source Reconstruction Results

Patient	Principal diagnosis	Lesion site	Delta activity (DA): Location of max. dipole density	Dipole density	Location of averaged epileptiform activity (SW)	GoF (%)	Same hemisphere		Same lobe		Distance to lesion margin (mm)	
							DA	SW	DA	SW	DA	SW
1	Embolized and partly resected vascular malformation	Left posterior insular cortex, left supramarginal + superior temporal gyrus	Supramarginal gyrus	524	Supramarginal gyrus	98.7	x	x	x	x	6	2
2	Resected meningioma, gliosis adjacent to resection hole and along the operative way of accession	Left temporopolar region and posterior insular cortex	Gray + white matter along interhemispheric fissure	994	Insular cortex	93.1	x	x		x	>46	14
3	Hippocampal atrophy	Left temporomesial cortex	No DA	—	Inferior temporal gyrus	97.2		x		x		36
4	Hippocampal sclerosis	Right temporomesial cortex	No DA	—	Middle occipitotemporal gyrus	95.0		x		x		22
5	Hippocampal sclerosis	Right temporomesial cortex	Middle orbital and parahippocampal gyrus	741	Semilunar gyrus	98.5	x	x	(x)	x	17	6
6	Defects and gliosis after contusio cerebri and subdural haematoma	Left temporal lobe	Inferior temporal gyrus	661	No SW	—	x		x		0	
7	Metastasis	Left superior and middle frontal gyrus	Superior frontal gyrus	3159	No SW	—	x		x		0	
8	Defect after intracerebral hemorrhage	Right lateral occipital gyrus	Angular gyrus	1315	No SW	—	x				9	
9	Hippocampal atrophy	Right temporomesial cortex	Uncus of opposite side	1230	Inferior temporal gyrus	95.7		x		x	37	28
10	Cerebral infarct	Posterior territory of the right middle cerebral artery	Angular gyrus	899	Superior temporal gyrus	96.5	x	x	x	x	0	0
11	Cerebral infarct	Posterior territory of the right middle cerebral artery	Precentral and postcentral gyrus	707	Supramarginal gyrus	97.0	x	x	(x)	x	3 and 0	0
12	Resected hemorrhagenic cavernoma	Left lateral occipital gyrus and left angular gyrus	No DA	—	Lateral occipital gyrus	97.3		x		x		7
13	Vascular malformation, gliosis of adjacent brain tissue	White matter of the right parietal lobe	No DA	—	White matter of parietal lobe	96.2		x		x		29
14	Protoplasmatic glioma	Left temporal lobe including hippocampus and amygdala	No DA	—	Insular cortex	97.5		x		x		15

Note. DA, delta activity; SW, interictal epileptiform activity, i.e., spikes or sharp waves.

region. At the time of this study, his MRI showed a large resection hole comprising parts of the left postcentral and supramarginal gyrus and residual embolized angiomatous tissue in the adjacent supramarginal and superior temporal gyrus. The EEG contained frequent sharp waves and dysrhythmic delta waves in the left temporal region. Both the maximum dipole density resulting from the source reconstruction of delta activity and the ECD location of the averaged interictal epileptiform activity were found in the supramarginal gyrus and within pathologically altered tissue near the resection hole (Fig. 2).

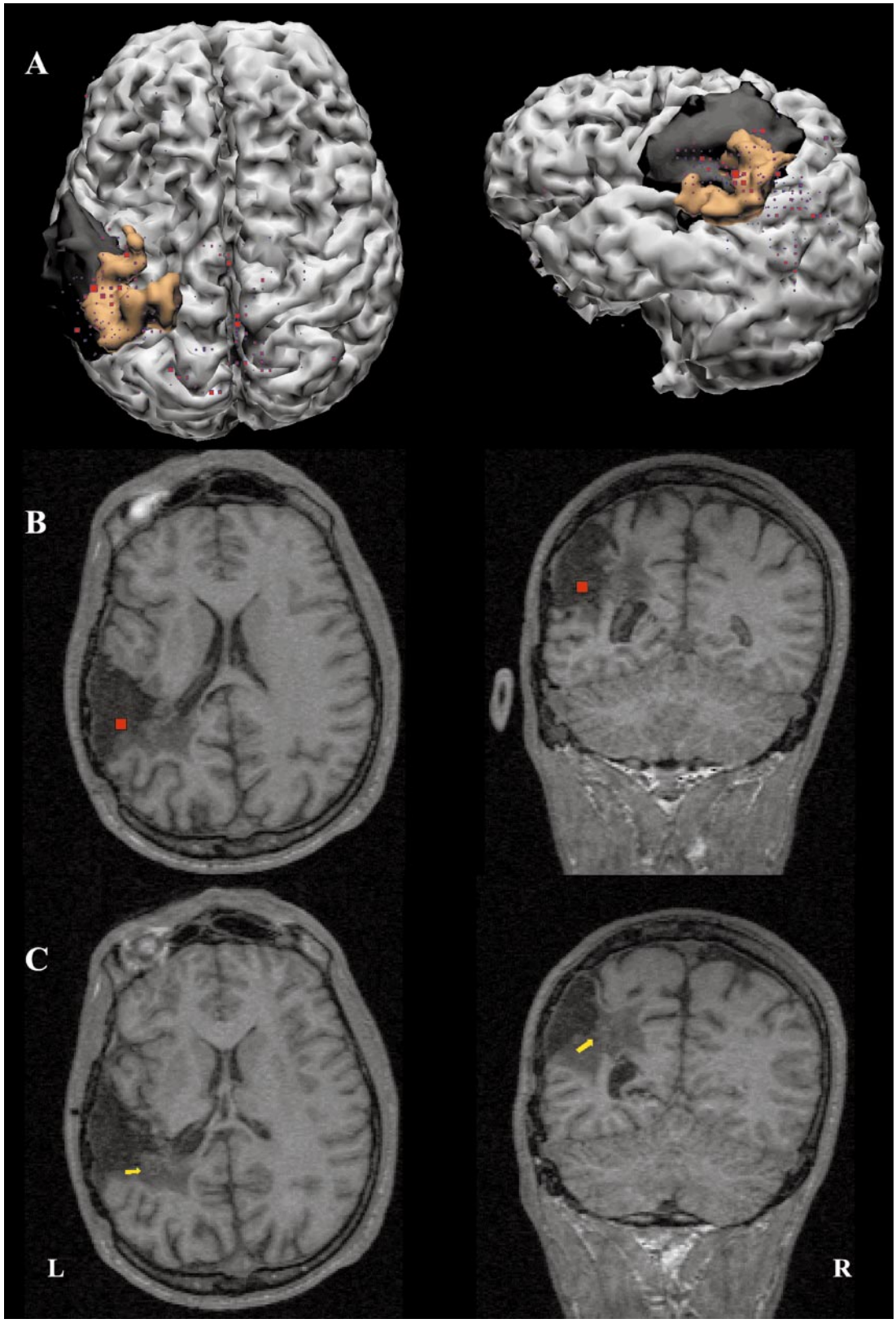

FIG. 2. Results of patient 1 (embolized and partly resected vascular malformation). (A) 3D view of the segmented cortex from above and from the side of the lesion. The segmented resection hole is shown in black, and the pathologically altered brain tissue in brown. The dipole density resulting from the source reconstruction of delta EEG activity is encoded in squares of different sizes which are projected onto the segmented cortex. The baseline offset is 10% of the maximum of the dipole density. (B) Maximum of the dipole density shown in axial and coronal slices of the patient's MRI. (C) ECD location corresponding to the averaged interictal epileptiform activity. The absolute size of arrows and squares in B and C carries no information.

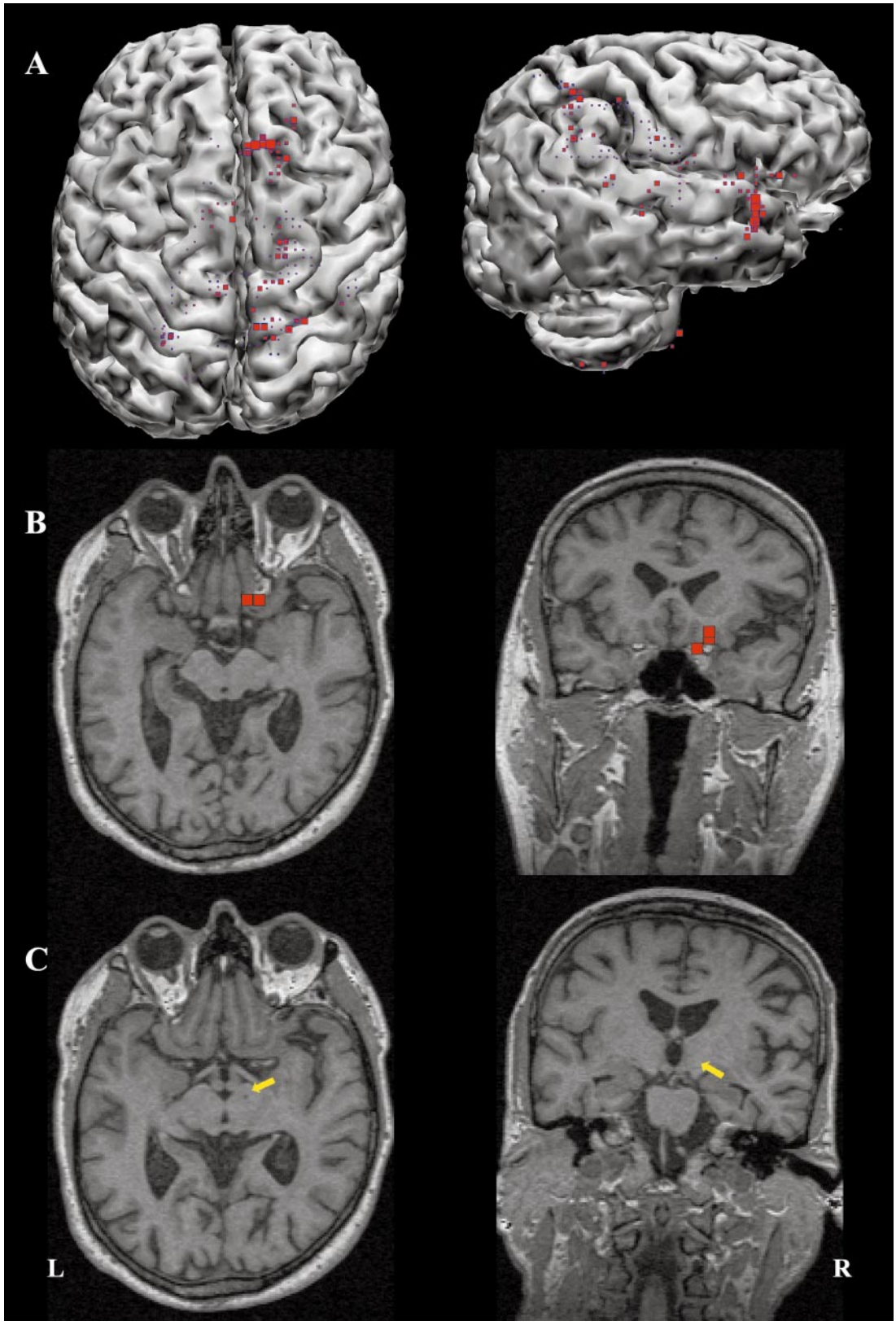

FIG. 3. Results of patient 5 (right hippocampal sclerosis). (A) Dipole density resulting from the source reconstruction of delta EEG activity projected onto the segmented cortex. The axial and coronal MRI slices are laid through the center of gravity of these localizations. (B) Maximum of the dipole density shown in axial and coronal MRI slices. (C) ECD location corresponding to the averaged interictal epileptiform activity.

Patient 5. This 51-year-old man with right hippocampal sclerosis suffered from pharmacoresistant epilepsy with epigastric auras and complex partial and secondarily generalized tonic–clonic seizures since the age of 4 years. The EEG contained intermittent delta waves, sharp waves, and sharp-slow waves in right frontal and temporal recordings. Video EEG monitoring showed a clear origin of ictal activity in the right sphenoidal electrode. Three days after recording the high-resolution EEG for this study, the patient underwent selective right amygdalohippocampectomy and remained seizure free since then. Source reconstruction of delta EEG activity yielded three equal maxima of the dipole density lying close together in the posterior part of the middle orbital gyrus and adjacent to the ipsilateral parahippocampal gyrus. The averaged interictal epileptiform activity was located in the right semilunar gyrus, i.e., adjacent to the amygdaloid nucleus (Fig. 3).

Patient 10. This 60-year-old woman had simple partial seizures with left-sided sensorimotor symptoms and secondarily generalized seizures after an infarction of the right middle cerebral artery. The MRI showed the infarct comprising the inferior parietal lobulus and parts of the angular and superior temporal gyrus. The EEG contained almost continuous delta waves and intermittent sharp waves in the right temporal and parietooccipital region. Source reconstruction of delta EEG activity resulted in three equal maxima of dipole density close together in the right angular gyrus along the infarct margin. The averaged interictal epileptiform activity was located in the right superior temporal gyrus and at the infarct margin as well (Fig. 4).

DISCUSSION

The purpose of this study was to investigate the accuracy of electric source reconstruction in patients with focal intracerebral lesions and epileptic seizures using an innovative approach: source reconstruction based on high-resolution EEG and considering the individual head anatomy as obtained from MRI.

Source Reconstruction of Delta EEG Activity

The present study is the first report of source reconstruction applied to focal delta *EEG* activity. The difficulty of such an approach lies in the possibility of multiple active sources, the relatively low signal-to-noise ratio (SNR), and the missing possibility to average this delta activity. Two methods, the PCA and the calculation of the dipole density, were used to overcome these problems and to handle multisource activity. A time-overlapping PCA analyzed the delta-filtered EEG data and preselected time epochs containing one predominant underlying source. The calculation of the dipole density resulted in a spatial average where concentrations of dipole locations were made visible while nonfocal activity averaged out (Kober *et al.,* 1992; Vieth *et al.,* 1996).

In 6 of 9 patients with focal delta EEG activity, the maximum of dipole density was found closer than 10 mm to the structural lesion, mostly at the immediate lesion border or within pathologically altered cortical tissue. Two of the remaining patients had right temporomesial lesions. The maxima of dipole density were found in the neighborhood of the affected hippocampus (posterior part of the middle orbital gyrus, adjacent to parahippocampal gyrus) and in the contralateral uncus hippocampi, respectively. It remains unclear whether these are really mislocalizations. In the first patient, one could speculate that the affected hippocampus influenced adjacent and via fornix frontoorbital neocortical tissue. In the other patient, the localization in the contralateral uncus could be a sign of dual pathology (So *et al.,* 1989; Cendes *et al.,* 1995). In one patient with operated left temporopolar meningioma, the location results were scattered around the interhemispheric fissure. Since the high-resolution EEG displayed only rare and flat delta waves the mislocalization seems to be a consequence of a low SNR which typically leads to erroneous dipole locations in the center of the head model.

The present results have to be assessed by comparing them with *MEG* source reconstruction results in literature. Vieth *et al.* (1996) investigated delta activity in 27 patients with different structural lesions. In all cases, the results of MEG source reconstruction were close to the lesion, mostly on the lesion margin. In 12 stroke patients, Kamada *et al.* (1997) located increased slow-wave activity adjacent to the infarcts. In the field of epilepsy, Gallen *et al.* (1997) found the localization of low-frequency neuromagnetic activity concordant with the presumed epileptogenic region in 48.5% of 33 investigated patients. Thereby, it was comparable to noninvasive ictal video EEG monitoring and was exceeded in specificity only by invasive ictal monitoring. A direct comparison between the results of this study and the aforementioned studies is not possible because of different patient populations and missing quantitative data about the distances between location results and structural lesions. However, the present results support the idea that source reconstruction based on high-resolution EEG or MEG can provide valuable information about the origin of abnormal delta activity.

What is the rationale of using focal delta activity as a marker of cortical dysfunction associated with epileptogenic cerebral lesions? Animal studies have shown that delta waves develop due to lesions of the thalamus or the white matter and are localized in the overlying cortex. It has been concluded that cerebral lesions can deprive the cortex of an adjusting influence from the white matter, which is responsible for main-

tenance of a normal basic activity (Gloor *et al.,* 1977; Schaul, 1990). Although the lesions do not have to be epileptogenic, a close association of focal slowing and focal epilepsy has been suggested (Quesney *et al.,* 1988; Panet-Raymond and Gotman, 1990; Blume *et al.,* 1993; Gambardella *et al.,* 1995). Gambardella *et al.* (1995), e.g., analyzed background abnormalities in 56 epilepsy patients with mesiotemporal atrophy. Delta waves and spikes occurred together in more than 85% of the cases, were never in disagreement with respect to lateralization, and showed a striking concordance concerning their location. Thus, delta activity can offer important additional localizing information about the epileptogenic focus.

Localizing delta activity has several advantages: In contrast to interictal or ictal epileptiform activity, delta activity does not need to be awaited or provoked by tapering off antiepileptic drugs. It is especially useful when interictal epileptiform activity is absent or very rare. It can be utilized as a screening tool for detecting cases in which pathological cortex is probably not confined to a focal region (Gallen *et al.,* 1997). Furthermore, source reconstruction could be applied to postictal slowing, a very reliable lateralizing finding according to Williamson *et al.* (1993) and Hufnagel *et al.* (1995).

Source Reconstruction of Interictal Epileptiform Activity

In all 11 patients with interictal epileptiform activity, the ECD locations were located in the same lobe as the MRI-verified lesion. In almost half of them, the ECD locations were closer than 10 mm to the nearest lesion margin. Thereby, the accuracy of source reconstruction was comparable with that of interictal and ictal dipole modeling described in literature (Stefan *et al.,* 1994; Boon and D'Have, 1995; Boon *et al.,* 1997; Diekmann *et al.,* 1998; Krings *et al.,* 1998; Minassian *et al.,* 1999; Herrendorf *et al.,* 2000). In all but 2 of 22 patients with temporal lobe epilepsy, Stefan *et al.* (1994) found the MEG results of epileptiform activity within the affected temporal lobe. In 7 of 8 patients with seizure-related tumors, the dipole location was within 10 mm of the lesion border. Diekmann *et al.* (1998) compared the localization of methohexital-induced spikes based on EEG, MEG, and combined EEG/MEG data. In 6 patients with a MRI-verified lesion, the EEG/MEG approach resulted in the smallest distances to the lesions (average, 18 mm) whereas MEG and EEG alone yielded larger values of 24 and 22 mm, respectively. Krings *et al.* (1998) located interictal EEG spike activity of 8 patients with mesiotemporal or extratemporal epileptogenic lesions to within 8 mm of the lesion margin. In 10 of 11 children with nonlesional extratemporal epilepsy, Minassian *et al.* (1999) found that the MEG location of epileptiform discharges corresponded to the ictal onset zone as established by intracranial recordings. Recently, Herrendorf *et al.* (2000) used source reconstruction based on a realistic head model (BEM) to locate interictal EEG activity in 5 patients with mesiotemporal epilepsy within a mean distance of 13.6 mm from the affected hippocampus.

What is the rationale of expecting the sources of interictal epileptiform activity close to focal epileptogenic lesions? The spatial relationship between epileptogenic lesion and irritative zone, i.e., the cortex area generating interictal spike activity, is complex (Engel, 1993; Lüders *et al.,* 1993). Interictal epileptiform activity may arise within the epileptogenic lesion (e.g., an infiltrative tumor), adjacent to it (e.g., in case of a noninfiltrating lesion like a cavernoma), or at a distance from it. Nevertheless, depth recordings and electrocorticograms (ECoG) have shown that epileptic activity often originates in brain tissue in the vicinity of focal lesions (Sutherling *et al.,* 1987; Palmini *et al.,* 1995). Considering the fact that in the present study interictal epileptiform activity was always located in the same lobe as the lesion, it seems unlikely that there was much contamination of the results by activity arising from irritative zones far away from the lesion.

In the present study, 3 of 4 patients showing a relatively large distance (22–36 mm) between location results and nearest lesion margin had a hippocampal atrophy or sclerosis. Their ECD locations did not appear in the affected hippocampus, but in adjacent temporal neocortex, i.e., the inferior temporal gyrus, or middle occipitotemporal gyrus. The reason could be that in cases of mesiotemporal lesions, epileptiform activity generated in the temporobasal or temporolateral cortex can mask the activity generated in deeper structures or that epileptiform activity is not "visible" for surface electrodes until it has propagated to adjacent neocortex. There is an ongoing debate whether surface electrodes can register electric fields generated in deep structures at amplitudes sufficient for source reconstruction (Gloor, 1985; Alarcon *et al.,* 1994; Krings *et al.,* 1998; Merlet *et al.,* 1998; Merlet and Gotman, 1999). According to Alarcon *et al.* (1994), physiologically unrealistic voltage gradients would be necessary for deep sources to evoke detectable scalp potentials. In contrast, Krings *et al.* (1998) found ECD locations in epileptogenic hippocampi and concluded that the calculations of Alarcon *et al.* might be true for dipolar *point* sources, but not for *distributed* sources which have a smaller decrease of the voltage gradient in relation to the distance from the source. Recently, Merlet and Gotman (1999) compared dipole locations based on scalp EEG paroxysms with intracerebral potentials recorded simultaneously. They never observed scalp EEG spikes corresponding to focal activity limited to mesiotemporal structures. In all instances, the lateral temporal neocortex at least was involved. Similarly, the results of neither the delta nor the epilepti-

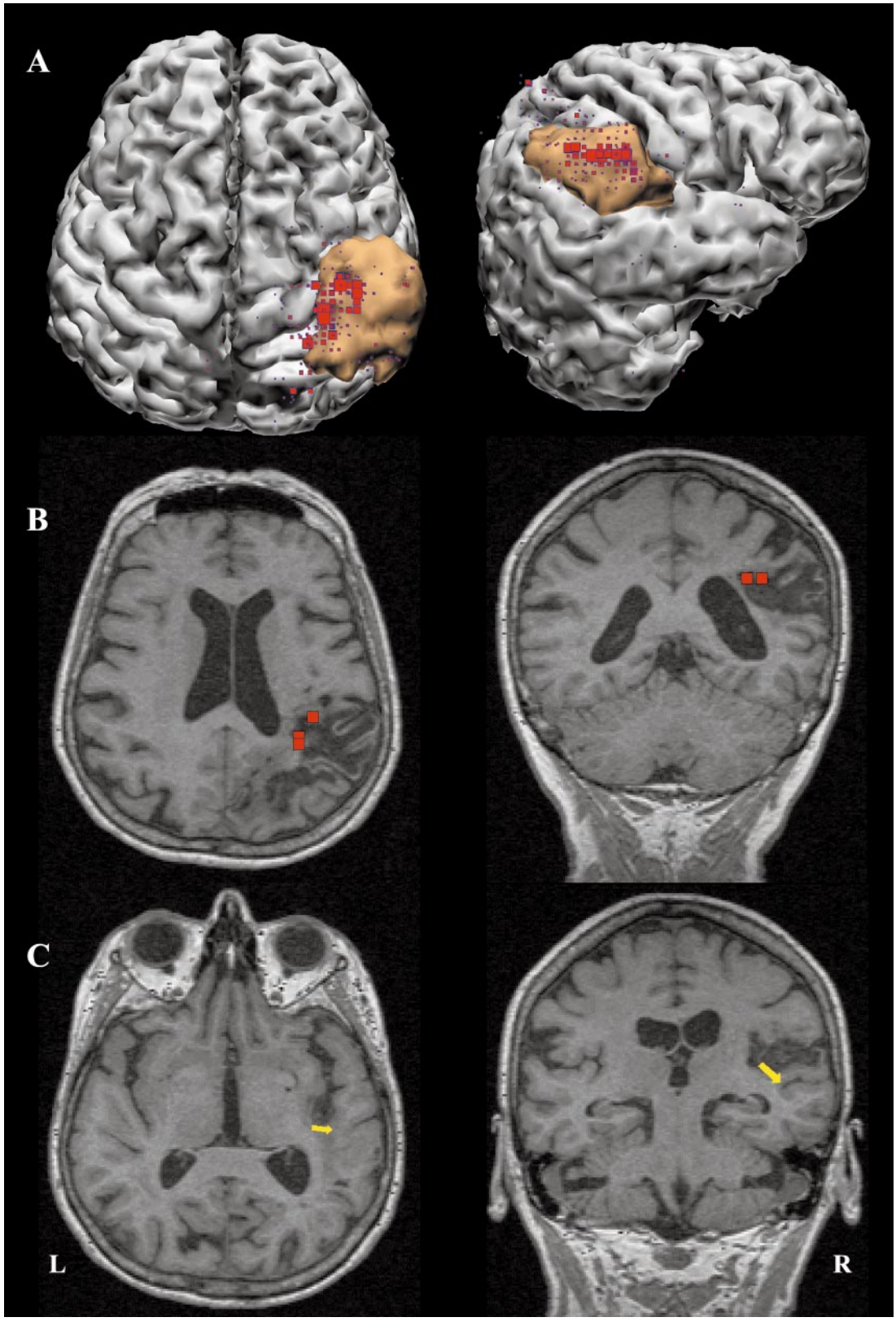

FIG. 4. Results of patient 10 (infarct in the posterior territory of the right middle cerebral artery). (A) Dipole density resulting from the source reconstruction of delta EEG activity projected onto the segmented cortex. The infarct area is shown in brown. (B) Maximum of the dipole density shown in axial and coronal MRI slices. (C) ECD location corresponding to the averaged interictal epileptiform activity.

form activity in this study were found in the hippocampus or amygdala. However, there were localization results in deep structures, e.g., uncus and inferior temporal gyrus.

The last of the four patients mentioned above had a venous malformation with gliosis of adjacent white matter of the right parietal lobe. The source of interictal epileptiform activity was located deep in the white matter. A possible explanation is that a single equivalent dipole characterizes only the center of mass and might be falsely located in the depth, when large brain areas are activated (Henderson *et al.,* 1975; Gloor, 1985).

To assess the results of this study and their clinical significance, the applied methodological steps and underlying assumptions are critically reviewed below:

On a typical adult head, the usual 21-channel "10/20" montage of electrodes has an interelectrode distance of about 6 cm. Better spatial sampling is the first requirement for extracting more detailed information from EEG (Gevins *et al.,* 1995). Increasing the number of electrodes to over 100 reduces the average interelectrode distance to about 2.5 cm. This is in the range of the typical cortex-to-scalp point-spread function, i.e., the size of the scalp representation of a small, discrete cortical source. On the other hand, the usefulness of increased spatial sampling is limited by the highly resistive skull acting like a low-pass filter for neuronal potentials and causing their distortion and smearing on the scalp (Gevins *et al.,* 1995). In view of these arguments, a high-resolution EEG based on about 60 scalp electrodes seems to be a reasonable compromise.

Assuming that focal spikes or sharp waves arise from a limited cortex area which is excited synchronously, a single equivalent current dipole was used for their source reconstruction. Since there are only six, i.e., three positional and three moment, parameters to determine the model has the advantage of being more stable than multiple dipole models (Mosher *et al.,* 1993). The high GoF values in this study indicated that the measured EEG potential distributions were congruent with the assumption of a single-dipole model. However, a single moving ECD model is a simplification. Even if the activation of a limited cortical area can be assumed and applying a single-dipole model seems to be adequate, one must keep in mind that the single ECD model applies to small focal sources and does not accurately characterize extended sources (Gallen *et al.,* 1997).

In spite of the short recording time and the fact that only *spontaneous* epileptiform activity was used to avoid any additional burden for the patients and to keep the method noninvasive in a strict sense, enough interictal epileptiform activity was recorded to yield reliable results of source reconstruction.

The coregistration of EEG and MRI data was based on matching digitized head surfaces as obtained by 3D ultrasound scanning and segmentation from the MRI data. This seems to be more reliable than matching a small number of reference points, because the digitization error of single points largely averages out when surfaces consisting of thousands of points are fitted (Pelizzari *et al.,* 1989; Kober *et al.,* 1993; Itti *et al.,* 1997). According to a previous study, the error of the localizing device was 1–2 mm within a distance of 1 m and the transformation error amounted to 1.6 mm on average which is smaller than the electrode diameter (Huppertz *et al.,* 1998).

EEG data strongly depend on the head's shape and its conductivities (Cohen *et al.,* 1990; Cuffin, 1990; Marin *et al.,* 1998). A three- or four-shell spherical head model is far from being physiological and seems to be an important cause of error in dipole modeling. Roth *et al.* (1993) found differences of source locations with three-sphere and realistically shaped head models which amounted to 1.97 cm on average. Source reconstruction results obtained with a realistically shaped head model were more in accordance with ECoG findings than results obtained with a three-sphere model (Roth *et al.,* 1997). On simulated EEG data, Yvert *et al.* (1997) showed that the best spherical model leads to localization errors of 5–6 mm in the upper part of the head and of 15–25 mm in the lower part. Therefore, a realistically shaped head model seems to be essential.

To summarize the results of delta EEG localization, a spatial dipole density distribution was calculated in a discrete, voxel-based manner similar to the original discrete dipole density plot (DDP) by Vieth *et al.* (1990). In comparison to a continuous DDP as developed later by Vieth *et al.* (1993) and improved by Diekmann *et al.* (1998), the usage of discrete volume units may produce a localization error of up to half of the edge length of the volume unit. However, the edge length of voxels was only 3 mm in this study instead of 10 mm in the discrete DDP of Vieth *et al.* (1990). Thus, the localization error due to discrete volume units could only be 1.5 mm at maximum.

Assessing the accuracy of electric source reconstruction necessarily must rest on the best available clinical and morphological data. In this study, the results of electric source reconstruction were validated by determining the distance to the nearest border of the structural lesion (Diekmann *et al.,* 1998; Krings *et al.,* 1998). This validation is based on the assumption that interictal epileptiform and focal delta EEG activity arise in the vicinity of the lesion. The reasons have been discussed above. But even with this assumption, the precise origin of the localized activity is not known, it remains open at which side of the lesion it is situated. The resulting possible error is in the range of the spatial extent of the lesion.

CONCLUSIONS

Epilepsy surgery requires the exact preoperative localization of the epileptogenic zone. There is no single method to localize and delineate the latter in its precise extension. The localization and determination of boundaries must derive from the convergence of different investigational methods (Lüders *et al.*, 1993).

Electric source reconstruction can be one of these methods. The results of the present study indicate that source reconstruction based on a high-resolution EEG and considering the individual head anatomy can localize abnormal slow and interictal epileptiform EEG activity with an adequate accuracy and a much finer spatial resolution than conventional scalp EEG.

The method may help to delineate both the irritative zone and the regions of cortical dysfunction. It can prove the epileptogenic nature of a structural lesion or guide the placement of intracranial electrodes when necessary (Krings *et al.*, 1998). On the other hand, it may increase confidence in the localization of the epileptogenic zone and thereby obviate the need for invasive recordings. The source reconstruction of focal delta activity can be especially useful when interictal epileptiform activity is absent, and it may provide an early indication of multifocal or bilateral pathology (Gallen *et al.*, 1997).

In conclusion, the method of electric source reconstruction applied to both abnormal slow and interictal epileptiform EEG activity seems to be a valuable additional noninvasive component in the multimodal presurgical evaluation of epilepsy patients.

ACKNOWLEDGMENTS

The authors thank Professor Dr. W. Berger, Professor Dr. B. Landwehrmeyer, and Dr. A. Schulze-Bonhage (University of Freiburg, Germany) for their helpful comments on the manuscript. The study was partly supported by a DFG grant (KR 1392/7-1).

REFERENCES

Alarcon, G., Guy, C. N., Binnie, C. D., Walker, S. R., Elwes, R. D., and Polkey, C. E. 1994. Intracerebral propagation of interictal activity in partial epilepsy: implications for source localisation. *J. Neurol. Neurosurg. Psychiatry* **57:** 435–449.

Baumgartner, C., Lindinger, G., Ebner, A., Aull, S., Serles, W., Olbrich, A., Lurger, S., Czech, T., Burgess, R., and Lüders, H. O. 1995. Propagation of interictal epileptic activity in temporal lobe epilepsy. *Neurology* **45:** 118–122.

Blume, W. T., Borghesi, J. L., and Lemieux, J. F. 1993. Interictal indices of temporal seizure origin. *Ann. Neurol.* **34:** 703–709.

Boon, P., D'Have, M., Adam, C., Vonck, K., Baulac, M., De Vandekerckhove, T., and De Reuck, J. 1997. Dipole modeling in epilepsy surgery candidates. *Epilepsia* **38:** 208–218.

Boon, P., and D'Have, M. 1995. Interictal and ictal dipole modelling in patients with refractory partial epilepsy. *Acta Neurol. Scand.* **92:** 7–18.

Buchner, H., Waberski, T. D., Fuchs, M., Wischmann, H. A., Wagner, M., and Drenckhahn, R. 1995. Comparison of realistically shaped boundary-element and spherical head models in source localization of early somatosensory evoked potentials. *Brain Topogr.* **8:** 137–143.

Cendes, F., Cook, M. J., Watson, C., Andermann, F., Fish, D. R., Shorvon, S. D., Bergin, P., Free, S., Dubeau, F., and Arnold, D. L. 1995. Frequency and characteristics of dual pathology in patients with lesional epilepsy. *Neurology* **45:** 2058–2064.

Chatrian, G. E., Bergamini, L., Dondey, M., Klass, D. W., Lennox-Buchtal, M., and Petersen, I. 1974. A glossary of terms most commonly used by clinical electroencephalographers. *Electroencephalogr. Clin. Neurophysiol.* **37:** 538–548.

Cohen, D., Cuffin, B. N., Yunokuchi, K., Maniewski, R., Purcell, C., Cosgrove, G. R., Ives, J., Kennedy, J. G., and Schomer, D. L. 1990. MEG versus EEG localization test using implanted sources in the human brain. *Ann. Neurol.* **28:** 811–817.

Cohen, D., and Cuffin, B. N. 1983. Demonstration of useful differences between magnetoencephalogram and electroencephalogram. *Electroencephalogr. Clin. Neurophysiol.* **56:** 38–51.

Cuffin, B. N. 1985. A comparison of moving dipole inverse solutions using EEG's and MEG's. *IEEE Trans. Biomed. Eng.* **32:** 905–910.

Cuffin, B. N. 1990. Effects of head shape on EEG's and MEG's. *IEEE Trans. Biomed. Eng.* **37:** 44–52.

Cuffin, B. N., Cohen, D., Yunokuchi, K., Maniewski, R., Purcell, C., Cosgrove, G. R., Ives, J., Kennedy, J., and Schomer, D. 1991. Tests of EEG localization accuracy using implanted sources in the human brain. *Ann. Neurol.* **29:** 132–138.

Diekmann, V., Becker, W., Jurgens, R., Grozinger, B., Kleiser, B., Richter, H. P., and Wollinsky, K. H. 1998. Localisation of epileptic foci with electric, magnetic and combined electromagnetic models. *Electroencephalogr. Clin. Neurophysiol.* **106:** 297–313.

Ebersole, J. S. 1994. Non-invasive localization of the epileptogenic focus by EEG dipole modeling. *Acta Neurol. Scand.* **152:** 20–28.

Engel, J., Jr., Rausch, R., Lieb, J. P., Kuhl, D. E., and Crandall, P. H. 1981. Correlation of criteria used for localizing epileptic foci in patients considered for surgical therapy of epilepsy. *Ann. Neurol.* **9:** 215–224.

Engel, J., Jr. 1993. Intracerebral recordings: organization of the human epileptogenic region. *J. Clin. Neurophysiol.* **10:** 90–98.

Friston, K. J., Stephan, K. M., Heather, J. D., Frith, C. D., Ioannides, A. A., Liu, L. C., Rugg, M. D., Vieth, J., Keber, H., Hunter, K., and Frackowiak, R. S. 1996. A multivariate analysis of evoked responses in EEG and MEG data. *NeuroImage* **3:** 167–174.

Fuchs, M., Wischmann, H. A., Wagner, M., and Theissen, A. 1998. Performance of realistically shaped boundary element method volume conductor models. In *BIOMAG98 Abstracts*, Abstract 86.

Gallen, C. C., Tecoma, E., Iragui, V., Sobel, D. F., Schwartz, B. J., and Bloom, F. E. 1997. Magnetic source imaging of abnormal low-frequency magnetic activity in presurgical evaluations of epilepsy. *Epilepsia* **38:** 452–460.

Gambardella, A., Gotman, J., Cendes, F., and Andermann, F. 1995. Focal intermittent delta activity in patients with mesiotemporal atrophy: A reliable marker of the epileptogenic focus. *Epilepsia* **36:** 122–129.

Geddes, L. A., and Baker, L. E. 1967. The specific resistance of biological material—A compendium of data for the biomedical engineer and physiologist. *Med. Biol. Eng.* **5:** 271–293.

Gevins, A., Brickett, P., Costales, B., Le, J., and Reutter, B. 1990. Beyond topographic mapping: Towards functional-anatomical imaging with 124-channel EEGs and 3-D MRIs. *Brain Topogr.* **3:** 53–64.

Gevins, A., Leong, H., Smith, M. E., Le, J., and Du, R. 1995. Mapping cognitive brain function with modern high-resolution electroencephalography. *Trends Neurosci.* **18:** 429–436.

Gloor, P., Ball, G., and Schaul, N. 1977. Brain lesions that produce delta waves in the EEG. *Neurology* **27:** 326–333.

Gloor, P. 1985. Neuronal generators and the problem of localization in electroencephalography: Application of volume conductor theory to electroencephalography. *J. Clin. Neurophysiol.* **2:** 327–354.

Henderson, C. J., Butler, S. R., and Glass, A. 1975. The localization of equivalent dipoles of EEG sources by the application of electrical field theory. *Electroencephalogr. Clin. Neurophysiol.* **39:** 117–130.

Herrendorf, G., Steinhoff, B. J., Kolle, R., Baudewig, J., Waberski, T. D., Buchner, H., and Paulus, W. 2000. Dipole-source analysis in a realistic head model in patients with focal epilepsy. *Epilepsia* **41:** 71–80.

Hufnagel, A., Poersch, M., Elger, C. E., Zentner, J., Wolf, H. K., and Schramm, J. 1995. The clinical and prognostic relevance of the postictal slow focus in the electrocorticogram. *Electroencephalogr. Clin. Neurophysiol.* **94:** 12–18.

Huppertz, H. J., Otte, M., Grimm, C., Kristeva-Feige, R., Mergner, T., and Lücking, C. H. 1998. Estimation of the accuracy of a surface matching technique for registration of EEG and MRI data. *Electroencephalogr. Clin. Neurophysiol.* **106:** 409–415.

Itti, L., Chang, L., Mangin, J. F., Darcourt, J., and Ernst, T. 1997. Robust multimodality registration for brain mapping. *Hum. Brain Map.* **5:** 3–17.

Kamada, K., Saguer, M., Moller, M., Wicklow, K., Katenhauser, M., Kober, H., and Vieth, J. 1997. Functional and metabolic analysis of cerebral ischemia using magnetoencephalography and proton magnetic resonance spectroscopy. *Ann. Neurol.* **42:** 554–563.

Kober, H., Vieth, J., Grummich, P., Daun, A., Weise, E., and Pongratz, H. 1992. The factor analysis used to improve the dipole-density-plot (DDP) to localize focal concentrations of spontaneous magnetic brain activity. *Biomed. Eng. (Berlin)* **37:** 164–165.

Kober, H., Grummich, P., and Vieth, J. 1993. Precise fusion of MEG and MRI tomography using a surface fit. *Biomed. Eng. (Berlin)* **38:** 355–356.

Koles, Z. J. 1998. Trends in EEG source localization. *Electroencephalogr. Clin. Neurophysiol.* **106:** 127–137.

Krings, T., Chiappa, K. H., Cuffin, B. N., Buchbinder, B. R., and Cosgrove, G. R. 1998. Accuracy of electroencephalographic dipole localization of epileptiform activities associated with focal brain lesions. *Ann. Neurol.* **44:** 76–86.

Kristeva-Feige, R., Grimm, C., Huppertz, H. J., Otte, M., Schreiber, A., Jager, D., Feige, B., Buchert, M., Hennig, J., Mergner, T., and Lücking, C. H. 1997. Reproducibility and validity of electric source localisation with high-resolution electroencephalography. *Electroencephalogr. Clin. Neurophysiol.* **103:** 652–660.

Lagerlund, T. D., Sharbrough, F. W., and Busacker, N. E. 1997. Spatial filtering of multichannel electroencephalographic recordings through principal component analysis by singular value decomposition. *J. Clin. Neurophysiol.* **14:** 73–82.

Leahy, R. M., Mosher, J. C., Spencer, M. E., Huang, M. X., and Lewine, J. D. 1998. A study of dipole localization accuracy for MEG and EEG using a human skull phantom. *Electroencephalogr. Clin. Neurophysiol.* **107:** 159–173.

Lüders, H. O., Engel, J., Jr., and Munari, C. 1993. General Principles. In *Surgical Treatment of the Epilepsies* (J. Engel, Ed.), pp. 137–153. Raven Press, New York.

Marin, G., Guerin, C., Baillet, S., Garnero, L., and Meunier, G. 1998. Influence of skull anisotropy for the forward and inverse problem in EEG: Simulation studies using FEM on realistic head models. *Hum. Brain Map.* **6:** 250–269.

Merlet, I., Garcia-Larrea, L., Ryvlin, P., Isnard, J., Sindou, M., and Mauguiere, F. 1998. Topographical reliability of mesio-temporal sources of interictal spikes in temporal lobe epilepsy. *Electroencephalogr. Clin. Neurophysiol.* **107:** 206–212.

Merlet, I., and Gotman, J. 1999. Reliability of dipole models of epileptic spikes. *Clin. Neurophysiol.* **110:** 1013–1028.

Minassian, B. A., Otsubo, H., Weiss, S., Elliott, I., Rutka, J. T., and Snead, O. C., 3rd 1999. Magnetoencephalographic localization in pediatric epilepsy surgery: Comparison with invasive intracranial electroencephalography. *Ann. Neurol.* **46:** 627–633.

Mosher, J. C., Spencer, M. E., Leahy, R. M., and Lewis, P. S. 1993. Error bounds for EEG and MEG dipole source localization. *Electroencephalogr. Clin. Neurophysiol.* **86:** 303–321.

Nakasato, N., Levesque, M. F., Barth, D. S., Baumgartner, C., Rogers, R. L., and Sutherling, W. W. 1994. Comparisons of MEG, EEG, and ECoG source localization in neocortical partial epilepsy in humans. *Electroencephalogr. Clin. Neurophysiol.* **91:** 171–178.

Palmini, A., Gambardella, A., Andermann, F., Dubeau, F., da Costa, J. C., Olivier, A, Tampieri, D., Gloor, P., Quesney, F., Andermann, E., *et al.* 1995. Intrinsic epileptogenicity of human dysplastic cortex as suggested by corticography and surgical results. *Ann. Neurol.* **37:** 476–487.

Panet-Raymond, D., and Gotman, J. 1990. Asymmetry in delta activity in patients with focal epilepsy. *Electroencephalogr. Clin. Neurophysiol.* **75:** 474–481.

Pelizzari, C. A., Chen, G. T., Spelbring, D. R., Weichselbaum, R. R., and Chen, C. T. 1989. Accurate three-dimensional registration of CT, PET, and/or MR images of the brain. *J. Comput. Assist. Tomogr.* **13:** 20–26.

Press, W. H., Teukolsky, S. A., Vetterling, W. T., and Flannery, B. P. 1992. Singular value decomposition. In *Numerical Recipes in C: The Art of Scientific Computing* (W. H. Press, Ed.), pp. 59–71. Cambridge Univ. Press, Cambridge.

Quesney, L. F., Abou-Khalil, B., Cole, A., and Olivier, A. 1988. Pre-operative extracranial and intracranial EEG investigation in patients with temporal lobe epilepsy: Trends, results and review of pathophysiologic mechanisms. *Acta Neurol. Scand. Suppl.* **117:** 52–60.

Roth, B. J., Balish, M., Gorbach, A., and Sato, S. 1993. How well does a three-sphere model predict positions of dipoles in a realistically shaped head? *Electroencephalogr. Clin. Neurophysiol.* **87:** 175–184.

Roth, B. J., Ko, D., von Albertini-Carletti, I. R., Scaffidi, D., and Sato, S. 1997. Dipole localization in patients with epilepsy using the realistically shaped head model. *Electroencephalogr. Clin. Neurophysiol.* **102:** 159–166.

Schaul, N. 1990. Pathogenesis and significance of abnormal nonepileptiform rhythms in the EEG. *J. Clin. Neurophysiol.* **7:** 229–248.

Scherg, M. 1990. Fundamentals of dipole source potential analysis. In *Advances in Audiology* (M. Hoke, Ed.), pp. 40–69. Karger, Basel.

So, N., Gloor, P., Quesney, L. F., Jones Gotman, M., Olivier, A., and Andermann, F. 1989. Depth electrode investigations in patients with bitemporal epileptiform abnormalities. *Ann. Neurol.* **25:** 423–431.

Soong, A. C., and Koles, Z. J. 1995. Principal-component localization of the sources of the background EEG. *IEEE Trans. Biomed. Eng.* **42:** 59–67.

Spencer, S. S., So, N. K., Engel, J., Williamson, P. D., Levesque, M. F., and Spencer, D. D. 1993. Depth electrodes. In *Surgical Treatment of the Epilepsies* (J. Engel, Ed.), pp. 359–375. Raven Press, New York.

Stefan, H., Schuler, P., Abraham Fuchs, K., Schneider, S., Gebhardt, M., Neubauer, U., Hummel, C., Huk, W. J., and Thierauf, P. 1994. Magnetic source localization and morphological changes in temporal lobe epilepsy: Comparison of MEG/EEG, ECoG and volumetric

MRI in presurgical evaluation of operated patients. *Acta Neurol. Scand. Suppl.* **152:** 83–88.

Sutherling, W. W., Crandall, P. H., Engel, J., Jr., Darcey, T. M., Cahan, L. D., and Barth, D. S. 1987. The magnetic field of complex partial seizures agrees with intracranial localizations. *Ann. Neurol.* **21:** 548–558.

Vieth, J., Grummich, P., Sack, G., Kober, H., Schneider, S., Abraham Fuchs, K., Kerber, U., Ganslandt, O., and Schmidt, T. 1990. Three dimensional localization of the pathological area in cerebro-vascular accidents with multichannel magnetoencephalography. *Biomed. Tech. Berlin* **35**(Suppl. 2): 238–239.

Vieth, J., Sack, G., Kober, H., Friedrich, S., Moeger, A., Weise, E., and Daun, A. 1993. The dipole density plot (DDP), a technique to show concentrations of dipoles. *Physiol. Meas.* **14**(Suppl. 4A): A41–A44.

Vieth, J. B., Kober, H., and Grummich, P. 1996. Sources of spontaneous slow waves associated with brain lesions, localized by using the MEG. *Brain Topogr.* **8:** 215–221.

Wagner, M., Fuchs, M., Wischmann, H. A., Ottenberg, K., and Dösel, O. 1995. Cortex segmentation from 3D MR images for MEG reconstructions. In *Biomagnetism: Fundamental Research and Clinical Applications* (C. Baumgartner, Ed.), pp. 433–438. Elsevier/IOS Press, Amsterdam.

Williamson, P. D., French, J. A., Thadani, V. M., Kim, J. H., Novelly, R. A., Spencer, S. S., Spencer, D. D., and Mattson, R. H. 1993. Characteristics of medial temporal lobe epilepsy. II. Interictal and ictal scalp electroencephalography, neuropsychological testing, neuroimaging, surgical results, and pathology. *Ann. Neurol.* **34:** 781–787.

Wong, P. K. 1993. The importance of source behavior in distinguishing populations of epileptic foci. *J. Clin. Neurophysiol.* **10:** 314–322.

Yvert, B., Bertrand, O., Thevenet, M., Echallier, J. F., and Pernier, J. 1997. A systematic evaluation of the spherical model accuracy in EEG dipole localization. *Electroencephalogr. Clin. Neurophysiol.* **102:** 452–459.